



HAL
open science

The impact of geomagnetic spikes on the production rates of cosmogenic ^{14}C and ^{10}Be in the Earth's atmosphere

Alexandre Fournier, Yves Gallet, Ilya Usoskin, Philip W Livermore, Gennady A Kovaltsov

► To cite this version:

Alexandre Fournier, Yves Gallet, Ilya Usoskin, Philip W Livermore, Gennady A Kovaltsov. The impact of geomagnetic spikes on the production rates of cosmogenic ^{14}C and ^{10}Be in the Earth's atmosphere. *Geophysical Research Letters*, 2015, 42 (8), pp.2759-2766. 10.1002/2015GL063461 . insu-01862970

HAL Id: insu-01862970

<https://insu.hal.science/insu-01862970>

Submitted on 28 Aug 2018

HAL is a multi-disciplinary open access archive for the deposit and dissemination of scientific research documents, whether they are published or not. The documents may come from teaching and research institutions in France or abroad, or from public or private research centers.

L'archive ouverte pluridisciplinaire **HAL**, est destinée au dépôt et à la diffusion de documents scientifiques de niveau recherche, publiés ou non, émanant des établissements d'enseignement et de recherche français ou étrangers, des laboratoires publics ou privés.

RESEARCH LETTER

10.1002/2015GL063461

Key Points:

- We model the impact of geomagnetic spikes on cosmogenic ^{14}C and ^{10}Be production
- A comparison is made against the observed cosmogenic nuclide records
- Our analysis does not allow confirmation of the two suggested geomagnetic spikes

Supporting Information:

- Readme
- Movie S2
- Movie S1

Correspondence to:

A. Fournier,
fournier@ipgp.fr

Citation:

Fournier, A., Y. Gallet, I. Usoskin, P. W. Livermore, and G. A. Kovaltsov (2015), The impact of geomagnetic spikes on the production rates of cosmogenic ^{14}C and ^{10}Be in the Earth's atmosphere, *Geophys. Res. Lett.*, 42, 2759–2766, doi:10.1002/2015GL063461.

Received 11 FEB 2015

Accepted 17 MAR 2015

Accepted article online 24 MAR 2015

Published online 24 APR 2015

Corrected 19 JUN 2015

This article was corrected on 19 JUN 2015. See end of the full text for details.

The impact of geomagnetic spikes on the production rates of cosmogenic ^{14}C and ^{10}Be in the Earth's atmosphere

Alexandre Fournier¹, Yves Gallet¹, Ilya Usoskin^{2,3}, Philip W. Livermore⁴, and Gennady A. Kovaltsov^{5,6}

¹Institut de Physique du Globe de Paris, Sorbonne Paris Cité, Université Paris Diderot, CNRS, Paris, France, ²Sodankylä Geophysical Observatory, University of Oulu, (Oulu), Finland, ³ReSoLVE Centre of Excellence, University of Oulu, (Oulu), Finland, ⁴School of Earth and Environment, University of Leeds, Leeds, UK, ⁵Ioffe Physical-Technical Institute, St. Petersburg, Russia, ⁶Institute of Physics of the Earth, Russian Academy of Sciences, Moscow, Russia

Abstract We seek corroborative evidence of the geomagnetic spikes detected in the Near East ca. 980 BC and 890 BC in the records of the past production rates of the cosmogenic nuclides ^{14}C and ^{10}Be . Our forward modeling strategy rests on global, time-dependent, geomagnetic spike field models feeding state-of-the-art models of cosmogenic nuclide production. We find that spike models with an energy budget in line with presently inferred large-scale flow at Earth's core surface fail to produce a visible imprint in the nuclide record. Spike models able to reproduce the intensity changes reported in the Near East require an unaccountably high-magnitude core flow, yet their computed impact on cosmogenic isotope production rates remains ambiguous. No simple and unequivocal agreement is obtained between the observed and modeled nuclide records at the epochs of interest. This indicates that cosmogenic nuclides cannot immediately be used to confirm the occurrence of these two geomagnetic spikes.

1. Introduction

The Earth's dynamo is a fascinating process which operates over a wide range of time scales (see, e.g., *Hulot et al.* [2010] and *Roberts and King* [2013], for recent reviews). Concealment by Earth's crust and mantle restricts observation of the variability of the geodynamo to time scales of ~ 1 year and larger. The so-called geomagnetic secular variation (GSV) takes the form of gentle fluctuations occasionally punctuated by extreme events, which are the subject of a growing interest within the communities of geomagnetism and paleo/archeomagnetism. These events have been highlighted by different data sets and have had different names ascribed (noting also that they may have distinct dynamical origins): for example, "geomagnetic jerks" were initially reported based on evidence seen in the East component of the GSV recorded in land-based observatories [*Courillot et al.*, 1978]. They occur on an annual time scale and their origin remains elusive (consult *Mandea et al.* [2010], for a review). Along similar lines, *Gallet et al.* [2003] termed "archeomagnetic jerks" abrupt changes in the millennial record of geomagnetic directions over Europe, apparently synchronous with relative intensity maxima. These changes are multidecadal, and they have been associated with episodes of high eccentricity of the geomagnetic dipole [*Gallet et al.*, 2009]. More recently, the concept of "geomagnetic spikes" has come to the fore, as a result of the archeomagnetic study of copper slag residues from the Near East by *Ben-Yosef et al.* [2009] and *Shaar et al.* [2011]. Analysis of the data suggests time rates of change of geomagnetic intensity as large as several $\mu\text{T}/\text{yr}$ sustained over a few decades, to contrast with the present-day maximum rate of $\sim 0.1 \mu\text{T}/\text{yr}$. *Livermore et al.* [2014] assessed the geophysical likelihood of these extreme events, by estimating core-surface flows able to sustain such dramatic changes. Their conclusion was that, if true, the reported occurrences of extreme intensity changes in the Near East records required a magnitude of core-surface flow 6–8 times larger than the commonly accepted value. However, *Livermore et al.* [2014] also pointed out that an explanation for spikes may lie beyond our current perception of core dynamics and the geodynamo, and highlighted the need for further corroborative evidence of such spikes. The goal of this letter is precisely to estimate whether it is possible to detect the impact of such spikes in other records spanning the past few millennia, namely, those of the production rates of the cosmogenic radionuclides ^{14}C and ^{10}Be (see, e.g., the review by *Beer et al.* [2012]). In the following, we describe in section 2 the methods we apply to estimate this impact, we present our results in section 3, and we discuss them in section 4.

2. Methods

We follow a two-step approach. First, we generate global, time-dependent models of the geomagnetic field $\mathbf{B}(t)$ that mimic the spikes reported in the Near East at epochs 980 BC and 890 BC [Ben-Yosef *et al.*, 2009; Shaar *et al.*, 2011]. Second, we use these field models to compute predictions of cosmogenic isotope ^{14}C and ^{10}Be production rates at these epochs, which are then compared with observational records.

2.1. Geomagnetic Field Models

In our approach, $\mathbf{B}(t)$ results from the superposition of a background reference field $\mathbf{B}_0(t)$ and of two perturbations, one per spike event. In the following, $\mathbf{B}_1^{\text{sp}}(t)$ (respectively $\mathbf{B}_2^{\text{sp}}(t)$) will refer to the spike field perturbation due to the 980 BC (respectively 890 BC) event, and T_1 (respectively T_2) will refer to epoch 980 BC (respectively 890 BC). The reference $\mathbf{B}_0(t)$ is the mean of the ensemble of 1000 A_FM archeomagnetic field models published by Licht *et al.* [2013]. In order to construct $\mathbf{B}_i^{\text{sp}}(t)$, we adopt the optimized core flow methodology of Livermore *et al.* [2014] and operate at Earth's core surface: for a given geomagnetic field configuration, and a given amount of available kinetic energy (specified in terms of an imposed root-mean-square velocity u_{rms}), this approach provides the optimal core flow $\mathbf{u}_i^{\text{opt}}$ that generates the fastest instantaneous rate of change of geomagnetic intensity, dF/dt , at a given site on Earth's surface (from now on the Timna-30 archeological site, with longitude $\varphi = 34.95^\circ\text{E}$ and latitude $\lambda = 29.77^\circ\text{N}$). In order to account for our uncertain knowledge of the geomagnetic field at the core surface and to build reliable statistics, we consider, at each T_i , 1000 different realizations of that field. For each realization, Gauss coefficients from spherical harmonic degree $\ell = 1$ to the truncation $L_B = 135$ [Livermore *et al.*, 2014] are specified as follows: coefficients from $\ell = 1$ to $\ell = 5$ are those of one member of the A_FM ensemble at epoch T_i (a different member for each realization). Degrees 6 to L_B are next populated following the stochastic method presented by Livermore *et al.* [2014].

We seek a purely toroidal $\mathbf{u}_i^{\text{opt}}$, truncated at spherical harmonic degree $L_u = 145$ [Livermore *et al.*, 2014] and consider two values for u_{rms} : $u_{\text{rms}} = 13$ km/yr, as indicated by present-day core flow studies [e.g., Holme, 2007, and references therein], and $u_{\text{rms}} = 65$ km/yr. We picked this second value in order to allow dF/dt to reach values of the order of $3 \mu\text{T/yr}$. Figure 1 illustrates this choice by means of the distribution of intensity changes obtained for the 1000 different field configurations for the 890 BC spike. With 1000 $\mathbf{u}_i^{\text{opt}}$ at hand, we construct the time dependency of $\mathbf{B}_i^{\text{sp}}(t)$ in the following way: We assume that each spike event lasts for 50 years, centered about epoch T_i and that during the first 25 years, the extra secular variation (ESV) due to the spike is governed by a steady $\mathbf{u}_i^{\text{opt}}$. The effect of the spike culminates at T_i , and during the next 25 years, the ESV is governed by $-\mathbf{u}_i^{\text{opt}}$. This piecewise-constant shape of the ESV allows the core to return to its normal mode of operation (that described by $\mathbf{B}_0(t)$) after 50 years. Although the prescribed time dependency is parameterized and not fully dynamically self-consistent, it should nevertheless suffice to estimate whether spikes can be detected in radionuclide records. Our geomagnetic models are finally obtained by taking the average of the 1000 models of $\mathbf{B}(t) = \mathbf{B}_0(t) + \mathbf{B}_1^{\text{sp}}(t) + \mathbf{B}_2^{\text{sp}}(t)$ so constructed. The two values of u_{rms} we use yield two models, hereafter referred to as M13 and M65, corresponding to $u_{\text{rms}} = 13$ km/yr and $u_{\text{rms}} = 65$ km/yr, respectively. Note that M65 produces spike events a bit less extreme than (but on par with) those described by Shaar *et al.* [2011], with dF/dt of $\sim 3 \mu\text{T/yr}$ instead of $\sim 4\text{--}5 \mu\text{T/yr}$ and a duration of 50 years instead of ~ 30 years.

2.2. Production of Cosmogenic Radionuclides

Cosmogenic radionuclides are produced in the Earth's atmosphere by cosmic rays which are the main source of such nuclides in the terrestrial system. The flux of cosmic rays is modulated in the heliosphere by variable solar activity. In addition, the geomagnetic field shields the Earth from cosmic rays, as often parameterized in terms of the geomagnetic cutoff rigidity [Cooke *et al.*, 1991]. Accordingly, geomagnetic fluctuations can potentially lead to observable variations in the production of cosmogenic radionuclides. After production and redistribution in the terrestrial system, they are stored in independently datable natural archives (tree trunks, ice cores, marine sediments, etc.). The two most useful nuclides are ^{14}C and ^{10}Be which have quite different distribution patterns: while ^{14}C takes part in the global carbon cycle and is globally mixed, ^{10}Be deposited in polar ice is only partly mixed [e.g., Beer *et al.*, 2012]. As a consequence, the global production of ^{14}C , denoted $Q(^{14}\text{C})$ henceforth, is predominantly sensitive to changes in the geomagnetic dipole moment, while the production and deposition of ^{10}Be , hereafter denoted $D(^{10}\text{Be})$, is affected by both the moment and the tilt of the dipole.

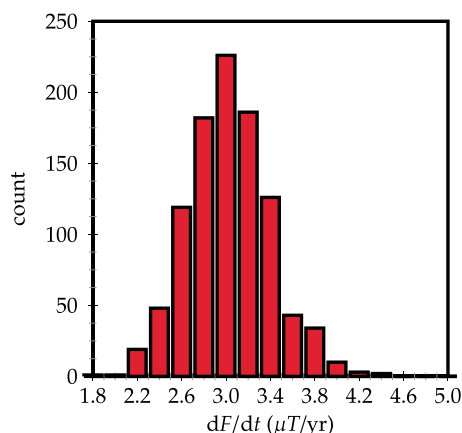


Figure 1. Distribution of the 1000 optimized archeomagnetic intensity changes at the location of Timna-30, for the 890 BC spike, assuming a root-mean-square core velocity u_{rms} equal to 65 km/yr. Bins of width 0.2 $\mu\text{T/yr}$.

We model production/deposition of the two nuclides as affected by the geomagnetic spikes under consideration. The production of ^{14}C is computed using the numerical model of *Kovaltsov et al.* [2012] in a way described elsewhere [*Usoskin et al.*, 2014]. The computed values of $Q(^{14}\text{C})$ are then compared with the ^{14}C production rates reconstructed by *Roth and Joos* [2013] from the tree-ring-based measurements of INTCAL-2009 [*Reimer et al.*, 2009]. In order to model data of ^{10}Be measured in polar ice, the ^{10}Be production is computed using the model of *Kovaltsov and Usoskin* [2010]. Transport and deposition of Beryllium is modeled according to a parameterization provided by *Heikkilä et al.* [2009] which is a full model of large-scale transport of ^{10}Be in a realistic modern atmosphere. However, there are empirical indications [*Bard et al.*, 1997; *McCracken*, 2004; *Usoskin et al.*, 2006] that a polar enhancement factor may play a role in the ^{10}Be data in comparison to predictions based on global transport, resulting in a higher polar variability of the signal. For the reference ^{10}Be deposition rate data, we use the GRIP

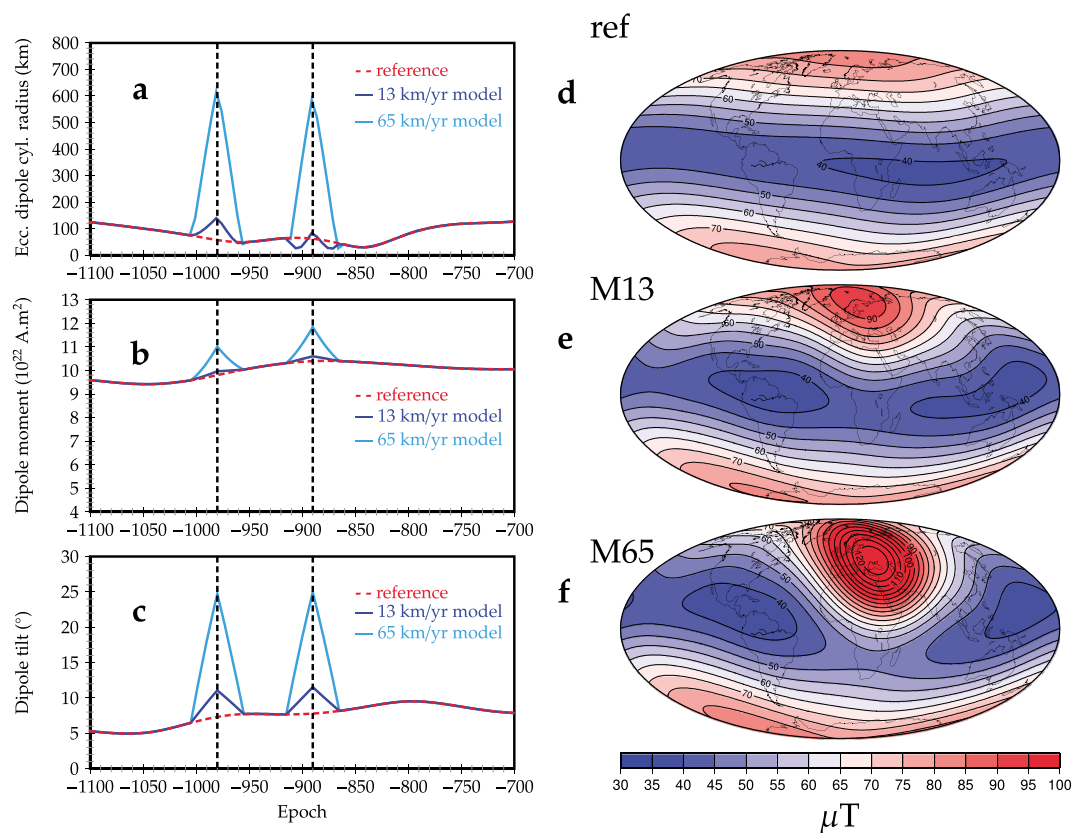


Figure 2. Properties of the geomagnetic models used in this study. (a) Cylindrical radius of the eccentric dipole as a function of time for three different archeomagnetic field models: in dashed red the A_FM reference model of *Licht et al.* [2013], and in blue and cyan, respectively, the M13 ($u_{rms} = 13 \text{ km/yr}$) and M65 ($u_{rms} = 65 \text{ km/yr}$) models developed in this study; see text for details. (b) Dipole moment and (c) dipole tilt evolution derived from the A_FM, M13 and M65 archeomagnetic field models (same color code as in Figure 2a). Vertical dashed lines indicate the assumed epochs of occurrence of the Near East spikes (980 BC and 890 BC). Intensity F of the geomagnetic field at Earth's surface at epoch 890 BC, for the (d) reference model, (e) model M13, and (f) model M65. Contours every 5 μT .

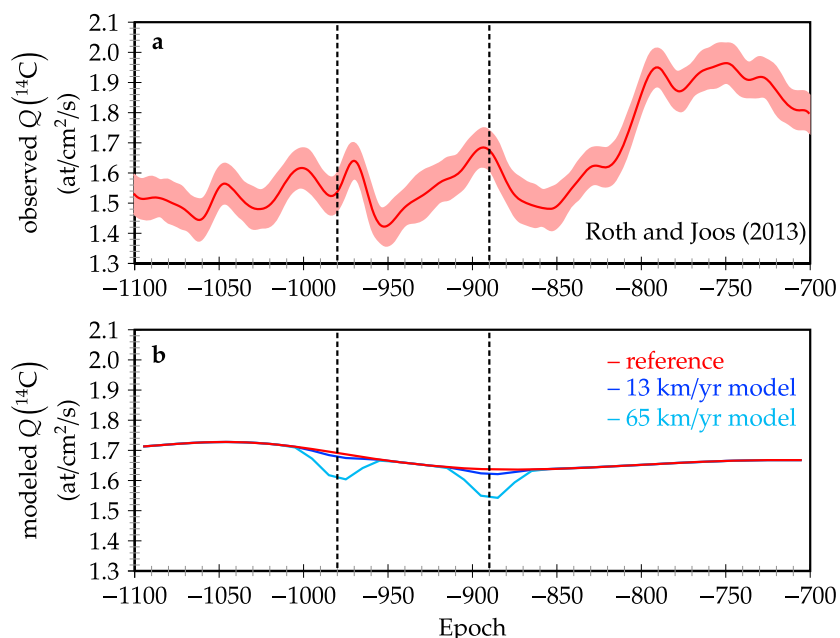


Figure 3. Variability of the ^{14}C production rate. (a) Observed ^{14}C production rates (along with ± 1 standard deviation) from 1100 BC to 700 BC according to Roth and Joos [2013]. (b) Impact of our geomagnetic models on $Q(^{14}\text{C})$, assuming a constant solar modulation potential $\phi = 500$ MV. Red: reference A_{FM} model. Blue: M13 model. Cyan: M65 model. Vertical dashed lines indicate the assumed epochs of occurrence of the Near East spikes (980 BC and 890 BC).

(Greenland Ice Core Project) ice core record obtained from Greenland [Yiou *et al.*, 1997]. We also show the EDML (Epica Dronning Maud Land) ^{10}Be record obtained from Antarctica [e.g., Ruth *et al.*, 2007; Steinhilber *et al.*, 2012], even though it presently does not rely on an ice model in contrast with the GRIP record (leading to ^{10}Be concentration data instead of depositional fluxes). Note that it is beyond the scope of this paper to comment on the respective reliability of the GRIP and EDML data sets, in particular, that concerning their dating.

In order to solely focus on the effect of the geomagnetic spikes on $Q(^{14}\text{C})$ and $D(^{10}\text{Be})$, we have assumed in the calculations constant solar activity at a moderate level, parameterized by a constant heliospheric modulation potential $\phi = 500$ MV (see, e.g., Usoskin *et al.* [2005], for its definition). The geomagnetic cutoff rigidity was calculated using the first eight Gauss spherical harmonic coefficients of the geomagnetic field decomposition in the eccentric dipole approximation [Fraser-Smith, 1987; Usoskin *et al.*, 2010].

3. Results

Figure 2 illustrates the geomagnetic field behavior associated with the occurrence of the two spikes. Figure 2a shows how the eccentricity varies among the two spike models and the reference between 1100 BC and 700 BC. Fluctuations of the cylindrical radius of the center of the eccentric dipole show, in particular, that model M65 is extreme, as it generates eccentricities of the order of ~ 500 km. Model M13, on the other hand, has a rather limited effect, with fluctuations of a few tens of kilometers. The occurrence of the two spikes induces two short-lasting increases in the dipole field moment, with different amplitudes depending on the model (Figure 2b). The effect is clearly minor for model M13. Figure 2c further illustrates the effect of spikes on the tilt of the dipole. While the reference level between ~ 1000 BC and ~ 850 BC is $\sim 5^\circ$, the dipole tilt reaches $\sim 10^\circ$ during the two spikes for model M13, increasing up to $\sim 25^\circ$ for model M65. The differences between the two models are further highlighted in Figures 2d–2f, where the geomagnetic intensity is plotted at the Earth's surface at epoch 890 BC for the reference model, model M13, and model M65 (see also Movies S1 and S2 in the supporting information for an animated illustration of the spike models).

Figure 3 shows the impact of our geomagnetic scenarios on $Q(^{14}\text{C})$ against the reference data provided by Roth and Joos [2013] for epochs comprised between 1100 BC and 700 BC. Figure 3a displays the observed

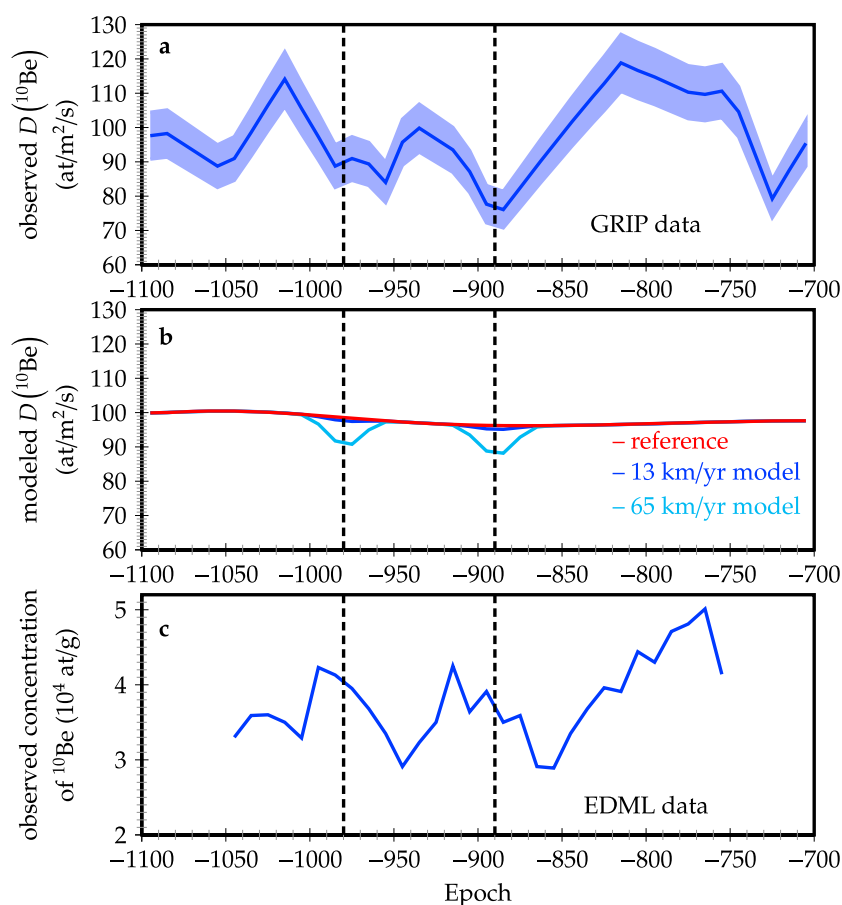


Figure 4. Variability of ^{10}Be in polar ice. (a) ^{10}Be deposition fluxes within the 1100–700 BC time interval obtained from the GRIP ice core [Yiou *et al.*, 1997]. (b) Modeled deposition of ^{10}Be , assuming a constant solar modulation potential $\phi = 500$ MV. Same notation as in Figure 3b. (c) ^{10}Be concentration data obtained from the EDML ice core record [e.g., Steinhilber *et al.*, 2012].

decadal variations in radiocarbon global production rate $Q(^{14}\text{C})$, whereas Figure 3b exhibits the expected changes in $Q(^{14}\text{C})$ induced by models M13 and M65. Both spikes drive a decrease in ^{14}C production rate, which is due to the concomitant increase in the dipole field moment (Figure 2b). Model M13 gives a practically negligible decrease, well within the uncertainties of $\pm(0.05\text{--}0.08)$ at/cm²/s estimated by Roth and Joos [2013]. For the M65 model, the spike-related decrease is about 0.1 at/cm²/s ($\sim 6\%$). This is slightly above the uncertainty level and may account for some of the fluctuations in the observed record during the tenth and ninth centuries BC, such as the dip occurring ca. 980 BC.

Figure 4 shows the comparison between the variations in $D(^{10}\text{Be})$ provided by the GRIP record (Figure 4a), the expected $D(^{10}\text{Be})$ derived from models M13 and M65 (Figure 4b), and the ^{10}Be concentration data from the EDML record (Figure 4c). We observe first that within the period of interest, the GRIP and EDML records exhibit a quite similar pattern of variations, marked by two major dips (a century apart), delayed by about 35 years in the EDML record with respect to the GRIP record. Concerning the modeled effects (Figure 4b), model M13 leads to a pair of very minor dips, with a relative decrease $\Delta D/D$ of approximately 1%. Model M65 induces a stronger signature, with $\Delta D/D \sim 10\%$, but this remains very close to the overall uncertainty level of ± 10 at/m²/s characterizing the GRIP record (note that uncertainty estimates are not presently available for the EDML record). Furthermore, our modeled fluctuations in ^{10}Be deposition are clearly of much smaller amplitude (about 1/3) than that of most fluctuations observed from GRIP. Note, however, that this discrepancy could be partly connected with the possible polar enhancement of ^{10}Be production not accounted for in the model (recall section 2.2).

4. Summary and Discussion

We have designed two simple models of the Iron Age geomagnetic spikes reported in the Near East in order to assess the imprint of these events on the production rates of cosmogenic nuclides ^{14}C and ^{10}Be . The two models, whose dynamics is admittedly simple, differ in the energy budget they are allocated: M13 is a conservative model, in line with our current understanding of core flow, but it is as such unable to sustain the rate of change of intensity dF/dt that can be inferred from the work of *Ben-Yosef et al.* [2009] and *Shaar et al.* [2011]. Model M65 requires core flows roughly 6–8 times stronger than is commonly accepted but is able to reproduce the reported dF/dt .

Both spike models induce a global effect on the production rates of radionuclides, because of the shielding by the geomagnetic field. This leads to a decrease of the production rate of radionuclides during the spike period. As an aside, it is worth mentioning that this effect, if not properly accounted for, would lead to a slight overestimate of the sunspot number reconstructed from cosmogenic radionuclides [see, e.g., *Usoskin et al.*, 2014]. We find that the modeled impact of M13 is too small to be above the noise level of both the ^{14}C and ^{10}Be records, indicating that its energy budget is too conservative for a successful search of any corroborative evidence of geomagnetic spikes.

The imprint of M65 is more significant. The impact on $Q(^{14}\text{C})$ is modeled to be about 6% of the mean production rate over the period of concern [*Roth and Joos*, 2013]; the impact is even stronger (about 10%) on $D(^{10}\text{Be})$. In both cases, however, the match between our models and the nuclide records remains ambiguous. Although it might appear that the ^{14}C record supplies corroborative evidence of the occurrence of the spike at 980 BC (Figure 3), no such agreement is observed for the 890 BC event. This may therefore cast some doubt on the occurrence of the 980 BC spike, and as a consequence, this would open to question the reliability of the high-resolution quasi-continuous archeointensity record reconstructed by *Shaar et al.* [2011]. The only apparent way of reconciling the real signal with the modeled one, assuming the existence of both spike events, is to admit the possibility that the dates T_1 and T_2 of the two spikes are in fact different, either younger by ~ 30 – 35 years ($T_1 \sim 945$ BC and $T_2 \sim 860$ BC, respectively) or older by for instance ~ 90 years than the dates proposed by *Shaar et al.* [2011] (yielding $T_1 \sim 1070$ BC and $T_2 \sim 980$ BC, respectively); but note that this solution is not unique if the spacing between the spikes can change, notwithstanding the possibility of an imprint of a third geomagnetic spike yet undetected in the 1070–980 BC time interval). Looking at the dating constraints described by these authors, relying on radiocarbon dates (the age interval for the Timna-30 site is comprised between 1109 BC and 836 BC at the 95% confidence level), depositional stratigraphy and on a simple age-height model assumed for the investigated slag mounds, such shifts in time seem possible. In the case of a shift toward younger dates, however, a major difficulty arises from the fact that the modeled effects would account for only about a half of the observed variability in the measured ^{14}C content over the studied period (Figure 3; note that this amplitude issue finds an echo in the ^{10}Be data, see below). This discrepancy would then indicate that the computations we performed in this study underestimate the effect of geomagnetic changes in cosmogenic data by a factor of ~ 2 , suggesting that some important physics is missing. Alternative options for reconciling the amplitudes of variations exist: one could widen the spatial extent of the spike events in our modeling, ascribing their origin to enhanced fluctuations of the dipole alone. One could also increase u_{rms} up to ~ 130 km/yr (leading to the possible occurrence of geomagnetic spikes even more extreme than those suggested in the Near East). Given our current state of knowledge of core processes and of spikes, neither option appears realistic.

A comparable difficulty also arises when comparing the observed and modeled $D(^{10}\text{Be})$ time series (Figures 4a and 4b). We might argue for the possibility of a corroborative evidence of the older spike ca. 980 BC, whose impact would induce a decadal fluctuation (superimposed on a secular trend) in $D(^{10}\text{Be})$. Regarding the younger spike (ca. 890 BC), though, even if both time series show a dip, the modeled variability amounts to only a third of the amplitude of the observed fluctuations. Even if this discrepancy may reflect, as previously mentioned, a missing polar enhancement in ^{10}Be modeling, a better match of the amplitudes could be obtained by shifting the dates of the two spikes backward, by ~ 80 – 90 years. Likewise, it is probable that the EDML data (Figure 4c) would lead, after suitable rescaling, to a similar discrepancy regarding the amplitudes of the measured and modeled variations. Furthermore, correlating the two major dips in EDML with the effect of the pair of spikes considered here would necessitate shifting T_1 and T_2 onward by ~ 35 years (Figures 4a and 4c), as in the case of the $Q(^{14}\text{C})$ records. As an interesting aside, a recent attempt to synchronize systematically the IntCal and Greenland ice core

time scales by *Muscheler et al.* [2014] indicates that, around 1000 BC, the GRIP data should indeed be shifted toward younger ages by about 25 years, thereby bringing it in line with the EDML and ^{14}C records. Seeking a correlation between these ^{10}Be -synchronized records and the possible imprint of the spikes would require in any case to shift (onward or backward) T_1 and T_2 (Figure 4).

Owing to the issues reported above, in particular, concerning the amplitude of the modeled impact of spikes and their exact timing, our study shows that the observed production rates of cosmogenic ^{14}C and ^{10}Be cannot immediately be used to confirm the occurrence of geomagnetic spikes. Consequently, it appears that only the acquisition of new high-quality and accurately dated archeointensity data will enable confirmation of the extreme geomagnetic field intensity variations proposed by *Ben-Yosef et al.* [2009] and *Shaar et al.* [2011]. Finally, geomagnetic spike events, if confirmed by further experimental studies, would then represent a clear challenge for our understanding of the geodynamo, making it necessary to put forward a suitable dynamical mechanism in Earth's core that could explain such rapid changes of geomagnetic intensity at Earth's surface.

Acknowledgments

We thank K. G. McCracken and an anonymous referee for their constructive comments. Numerical computations were partly performed on the S-CAPAD platform, IPGP, France. This work was partly supported by the French national program PNP/INSU and by IPGP visiting program. Support by the Academy of Finland to the ReSoLVE Center of Excellence (project 272157) is acknowledged. P.W.L. was supported by NERC grant NE/G014043/1. Y.G. and G.K. were partly financed by grant N 14.Z50.31.0017 of the Russian Ministry of Science and Education. Figures were generated using the LaTeX pstricks-add package and the generic mapping tools of *Wessel et al.* [2013]. IPGP contribution 3617. Requests for material and data should be addressed to A.F. (fournier@ipggp.fr).

The Editor thanks two anonymous reviewers for their assistance in evaluating this paper.

References

- Bard, E., G. M. Raisbeck, F. Yiou, and J. Jouzel (1997), Solar modulation of cosmogenic nuclide production over the last millennium: Comparison between ^{14}C and ^{10}Be records, *Earth Planet. Sci. Lett.*, *150*(3), 453–462, doi:10.1016/S0012-821X(97)00082-4.
- Beer, J., K. McCracken, and R. von Steiger (2012), *Cosmogenic Radionuclides*, Physics of Earth and Space Environments, Springer, Berlin, doi:10.1007/978-3-642-14651-0_9.
- Ben-Yosef, E., L. Tauxe, T. E. Levy, R. Shaar, H. Ron, and M. Najjar (2009), Geomagnetic intensity spike recorded in high resolution slag deposit in Southern Jordan, *Earth Planet. Sci. Lett.*, *287*(3), 529–539, doi:10.1016/j.epsl.2009.09.001.
- Cooke, D. J., J. E. Humble, M. A. Shea, D. F. Smart, N. Lund, I. L. Rasmussen, B. Byrnek, P. Goret, and N. Petrou (1991), On cosmic-ray cut-off terminology, *Il Nuovo Cimento C*, *14*(3), 213–234, doi:10.1007/BF02509357.
- Courtillot, V., J. Ducruix, and J.-L. Le Mouél (1978), Sur une accélération récente de la variation séculaire du champ magnétique terrestre, *C. R. Acad. Sci. D*, *287*, 1095–1098.
- Fraser-Smith, A. C. (1987), Centered and eccentric geomagnetic dipoles and their poles, 1600–1985, *Rev. Geophys.*, *25*(1), 1–16, doi:10.1029/RG025i001p00001.
- Gallet, Y., A. Genevey, and V. Courtillot (2003), On the possible occurrence of archaeomagnetic jerks in the geomagnetic field over the past three millennia, *Earth Planet. Sci. Lett.*, *214*(1), 237–242, doi:10.1016/S0012-821X(03)00362-5.
- Gallet, Y., G. Hulot, A. Chulliat, and A. Genevey (2009), Geomagnetic field hemispheric asymmetry and archeomagnetic jerks, *Earth Planet. Sci. Lett.*, *284*(1), 179–186, doi:10.1016/j.epsl.2009.04.028.
- Heikkilä, U., J. Beer, and J. Feichter (2009), Meridional transport and deposition of atmospheric ^{10}Be , *Atmos. Chem. Phys.*, *9*(2), 515–527, doi:10.5194/acp-9-515-2009.
- Holme, R. (2007), Large-scale flow in the core, in *Core Dynamics, Treatise on Geophysics*, vol. 8, edited by P. Olson and G. Schubert, pp. 107–130, Elsevier, Amsterdam.
- Hulot, G., C. C. Finlay, C. G. Constable, N. Olsen, and M. Mandea (2010), The magnetic field of planet Earth, *Space Sci. Rev.*, *152*, 159–222, doi:10.1007/s11214-010-9644-0.
- Kovaltsov, G. A., and I. G. Usoskin (2010), A new 3D numerical model of cosmogenic nuclide ^{10}Be production in the atmosphere, *Earth Planet. Sci. Lett.*, *291*(1), 182–188, doi:10.1016/j.epsl.2010.01.011.
- Kovaltsov, G. A., A. Mishev, and I. G. Usoskin (2012), A new model of cosmogenic production of radiocarbon ^{14}C in the atmosphere, *Earth Planet. Sci. Lett.*, *337*, 114–120, doi:10.1016/j.epsl.2012.05.036.
- Licht, A., G. Hulot, Y. Gallet, and E. Thébaud (2013), Ensembles of low degree archeomagnetic field models for the past three millennia, *Phys. Earth Planet. Inter.*, *224*, 38–67, doi:10.1016/j.pepi.2013.08.007.
- Livermore, P. W., A. Fournier, and Y. Gallet (2014), Core-flow constraints on extreme archeomagnetic intensity changes, *Earth Planet. Sci. Lett.*, *387*, 145–156, doi:10.1016/j.epsl.2013.11.020.
- Mandea, M., R. Holme, A. Pais, K. Pinheiro, A. Jackson, and G. Verbanac (2010), Geomagnetic jerks: Rapid core field variations and core dynamics, *Space Sci. Rev.*, *155*(1–4), 147–175, doi:10.1007/s11214-010-9663-x.
- McCracken, K. G. (2004), Geomagnetic and atmospheric effects upon the cosmogenic ^{10}Be observed in polar ice, *J. Geophys. Res.*, *109*, A04101, doi:10.1029/2003JA010060.
- Muscheler, R., F. Adolphi, and M. F. Knudsen (2014), Assessing the differences between the Intcal and Greenland ice-core time scales for the last 14,000 years via the common cosmogenic radionuclide variations, *Quat. Sci. Rev.*, *106*, 81–87, doi:10.1016/j.quascirev.2014.08.017.
- Reimer, P., et al. (2009), IntCal09 and Marine09 radiocarbon age calibration curves, 0–50,000 years cal BP, *Radiocarbon*, *51*(4), 1111–1150.
- Roberts, P. H., and E. M. King (2013), On the genesis of the Earth's magnetism, *Rep. Prog. Phys.*, *76*(9), 096801, doi:10.1088/0034-4885/76/9/096801.
- Roth, R., and F. Joos (2013), A reconstruction of radiocarbon production and total solar irradiance from the Holocene ^{14}C and CO_2 records: Implications of data and model uncertainties, *Clim. Past*, *9*(4), 1879–1909, doi:10.5194/cp-9-1879-2013.
- Ruth, U., et al. (2007), EDML1: A chronology for the EPICA deep ice core from Dronning Maud Land, Antarctica, over the last 150 000 years, *Clim. Past*, *3*(3), 475–484, doi:10.5194/cp-3-475-2007.
- Shaar, R., E. Ben-Yosef, H. Ron, L. Tauxe, A. Agnon, and R. Kessel (2011), Geomagnetic field intensity: How high can it get? How fast can it change? Constraints from Iron Age copper slag, *Earth Planet. Sci. Lett.*, *301*(1), 297–306, doi:10.1016/j.epsl.2010.11.013.
- Steinhilber, F., et al. (2012), 9,400 years of cosmic radiation and solar activity from ice cores and tree rings, *Proc. Nat. Acad. Sci.*, *109*(16), 5967–5971, doi:10.1073/pnas.1118965109.
- Usoskin, I. G., K. Alanko-Huotari, G. A. Kovaltsov, and K. Mursula (2005), Heliospheric modulation of cosmic rays: Monthly reconstruction for 1951–2004, *J. Geophys. Res.*, *110*, A12108, doi:10.1029/2005JA011250.
- Usoskin, I. G., S. K. Solanki, G. A. Kovaltsov, J. Beer, and B. Kromer (2006), Solar proton events in cosmogenic isotope data, *Geophys. Res. Lett.*, *33*, L08107, doi:10.1029/2006GL026059.

- Usoskin, I. G., I. A. Mironova, M. Korte, and G. A. Kovaltsov (2010), Regional millennial trend in the cosmic ray induced ionization of the troposphere, *J. Atmos. Sol. Terr. Phys.*, *72*(1), 19–25, doi:10.1016/j.jastp.2009.10.003.
- Usoskin, I. G., G. Hulot, Y. Gallet, R. Roth, A. Licht, F. Joos, G. A. Kovaltsov, E. Thébault, and A. Khokhlov (2014), Evidence for distinct modes of solar activity, *Astron. Astrophys.*, *562*, L10, doi:10.1051/0004-6361/201423391.
- Wessel, P., W. H. F. Smith, R. Scharroo, J. Luis, and F. Wobbe (2013), Generic mapping tools: Improved version released, *Eos Trans. AGU*, *94*(45), 409–410, doi:10.1002/2013EO450001.
- Yiou, F., et al. (1997), Beryllium 10 in the Greenland ice core project ice core at Summit, Greenland, *J. Geophys. Res.*, *102*(C12), 26,783–26,794, doi:10.1029/97JC01265.

Erratum

In the originally published version of this article, figure 4c was missing the scaling factor of 10^4 on the y axis. The scaling factor has since been added, and this version may be considered the authoritative version of record.